Journal of Materials Chemistry C

A p-π* Conjugated Triarylborane as an Alcohol-Processable n-Type Semiconductor for Organic Optoelectronic Devices

Journal:	*Journal of Materials Chemistry C*
Manuscript ID	TC-ART-03-2019-001562.R1
Article Type:	Paper
Date Submitted by the Author:	10-May-2019
Complete List of Authors:	Yu, Yingjian; Chinese Academy of Sciences, Changchun Institute of Applied Chemistry Dong, Changshuai; Changchun Institute of Applied Chemistry, Chinese Academy of Sciences Alahmadi, Abdullah; Rutgers University Newark Meng, Bin; Changchun Institute of Applied Chemistry, Chinese Academy of Sciences, Liu, Jun; Chinese Academy of Sciences, Changchun Institute of Applied Chemistry Jaekle, Frieder; Rutgers University Newark Wang, Lixiang; Changchun Institute of Applied Chemistry, Chinese Academy of Sciences

ARTICLE

A p-π* Conjugated Triarylborane as an Alcohol-Processable n-Type Semiconductor for Organic Optoelectronic Devices

Received 00th January 20xx,
Accepted 00th January 20xx

DOI: 10.1039/x0xx00000x

Yingjian Yu,†[ab] Changshuai Dong,†[ab] Abdullah F. Alahmadi,[c] Bin Meng,*[a] Jun Liu,*[a] Frieder Jäkle*[c] and Lixiang Wang[a]

We report a p-π* conjugated organic molecule based on triarylborane as n-type organic semiconductor with unique alcohol solubility. Its favorable alcohol solubility even in the absence of polar side chains is mainly due to the large dipole moment and enhanced flexibility of the conjugated backbone once the boron atom is embedded. The p-π* conjugation directly affects the electronic structure as the LUMO is fully delocalized, including the boron atom, whereas the HOMO has the boron atom residing on a node. As a result, the molecule exhibits low-lying LUMO/HOMO energy levels of -3.61 eV / -5.73 eV paired with a good electron mobility of 1.37×10^{-5} cm^2 V^{-1} s^{-1}. We further demonstrate its application as an electron acceptor in alcohol-processed organic solar cells (OSCs). To our best knowledge, this p-π* conjugated molecule is the first alcohol-processable non-fullerene electron acceptor, a feature that is in strong demand for environmentally friendly processing of OSCs.

Introduction

Both p-type and n-type organic semiconductors are required for organic optoelectronic applications, such as organic light emitting diodes (OLEDs), organic field-effect transistors (OFETs) and organic solar cells (OSCs).[1] The development of n-type organic semiconductors lags far behind that of the p-type counterparts.[2] Most n-type organic semiconductors are derived from π-conjugated molecules, in which carbon-carbon single bonds and double bonds alternate in the backbone.[3] Doping or modification with heteroatoms is an attractive approach to enhance the acceptor character of conjugated organic materials.[4] Thus, a new strategy to design n-type semiconductors for OSC applications involves p-π* conjugation with an electron-deficient boron atom. Representative examples of p-π* conjugated molecular and polymeric arylboranes are illustrated in Figure 1.[5] In these systems, the empty $2p_z$ orbital of the boron atom overlaps with the π* orbitals of aromatic units, endowing the arylboranes with strong acceptor characteristics.[6,7] Polymers **B** derived from hydroboration polymerization have been explored as components of OSCs in blends with P3HT.[5a,b] Recently, we have unambiguously demonstrated the n-type semiconductor properties of p-π* conjugated triarylborane polymers (**A**).[5c] Organic acceptor-substituted triarylborane small molecules such as **C** or **D** have also attracted significant attention for OSC and as luminescent sensors.[5d,e] In this manuscript, we report a new p-π* conjugated n-type organic small molecule based on triarylborane, which shows unique alcohol solubility even in the absence of polar side chains.[8] This alcohol solubility is very desirable for environmentally friendly processing in organic optoelectronic applications.[9]

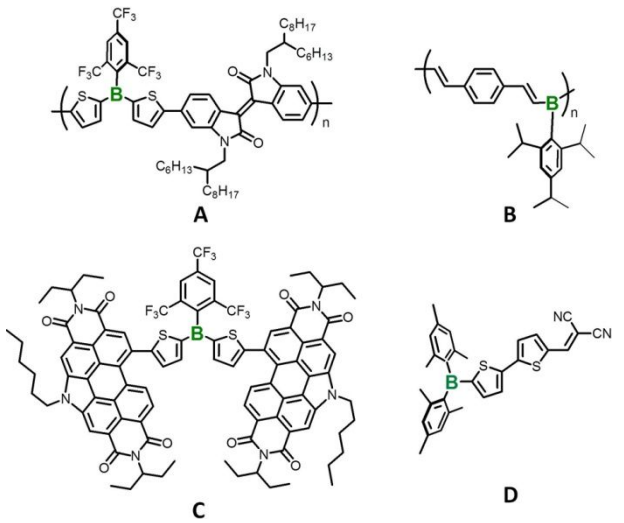

Figure 1. Examples of p-π* conjugated arylboranes.

Compared with inorganic semiconductors, one of the greatest advantages of organic materials is their solution-processability at low cost.[1] As typical π-conjugated molecules possess a rigid and hydrophobic backbone they tend to be

[a] State Key Laboratory of Polymer Physics and Chemistry, Changchun Institute of Applied Chemistry, Chinese Academy of Sciences, Changchun 130022 (P. R. China). E-mail: mengbin@ciac.ac.cn; liujun@ciac.ac.cn
[b] University of Science and Technology of China, Hefei 230026 (P. R. China)
[c] Department of Chemistry, Rutgers University - Newark, 73 Warren Street, Newark, NJ 07102 (USA), E-mail: fjaekle@rutgers.edu
† These authors contributed equally to this work.
Electronic Supplementary Information (ESI) available: [Experimental details, theoretical calculations, solubility, thermal property, mobility, morphology, as well as OSC device fabrications and characterizations]. See DOI: 10.1039/x0xx00000x

soluble in halogenated or aromatic solvents of low polarity,[10] but these solvents can be harmful to the environment and human body.[11] Conversely, they are generally insoluble in eco-friendly solvents, such as alcohols and water. For the large-scale manufacturing of organic optoelectronic devices, it is urgent to develop organic semiconductors with alcohol processability.[9] To render π-conjugated molecules soluble in alcohols, the general strategy has been to use polar or ionic side chains or substituents, such as oligo(ethylene glycol) (OEG) groups,[9a,b] phosphonate groups,[12] sulfonate groups,[13] ammonium groups,[14] etc.

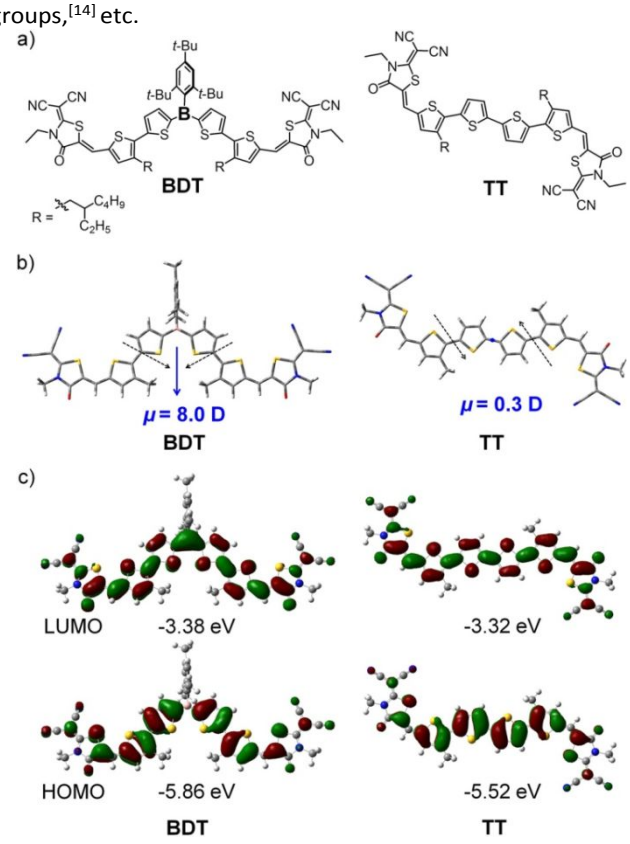

Figure 2. a) Chemical structures of **BDT** and **TT**. b) The optimized configurations and natural dipole moments and c) Kohn–Sham LUMOs/HOMOs and E_{LUMO}/E_{HOMO} of **BDT** and **TT** based on DFT calculation. All of the long alkyl chains have been replaced by methyl groups for simplification.

Herein, we realize the alcohol solubility of n-type organic semiconductors by embedding a boron atom into the conjugated backbone. Figure 2a shows the chemical structure of the alcohol-soluble n-type molecule, (2,4,6-tri-tert-butylphenyl)di(5-(2-((Z)-3-ethyl-5-((4-(2-ethylhexyl)thiophen-2-yl)methylene)-4-oxothiazolidin-2-ylidene)malononitrile)-thiophene-2-yl)borane (**BDT**). In **BDT**, the p-π* conjugated triarylborane core unit is end-capped by two electron-withdrawing 2-(3-ethyl-4-oxothiazolidin-2-ylidene)malono-nitrile groups.[15] The 2,4,6-tri-tert-butylphenyl (Mes*) group on boron serves as a bulky group that endows the molecule with excellent stability even in protic solvents. Although **BDT** has hydrophobic alkyl side chains, it is well soluble in alcohol solvents up to 9 mg/mL. Thus, we not only demonstrate the low-lying energy levels and favorable electron mobility of **BDT**, but also disclose its application as electron acceptor in alcohol-processed OSC devices. To our best knowledge, **BDT** is the first alcohol-processable non-fullerene electron acceptor for OSCs.[16]

Results and discussion

The synthetic route to **BDT** is illustrated in Scheme 1. The bromo-substituted end-capping group (**3**) was synthesized by Knoevenagel condensation of 5-bromo-4-(2-ethylhexyl)-thiophene-2-carbaldehyde (**2**) and 2-(3-ethyl-4-oxothiazolidin-2-ylidene)malononitrile. The distannylated triarylborane core unit (**4**) was prepared following our previously reported procedures.[6a,b] Finally, Stille coupling of **3** and **4** afforded the desired acceptor molecule, **BDT**. For comparison, we also synthesized the reference molecule without the boron atom, **TT** (Figure 2a). The chemical structure of **BDT** was confirmed by ^{1}H NMR, ^{13}C NMR, ^{11}B NMR and element analysis. Due to the bulky Mes* group on the boron atom **BDT** is highly stable under ambient conditions in the solid state and in solution. According to thermogravimetric analysis (TGA), **BDT** also shows good thermal stability with a high degradation temperature (T_d) at 5% weight loss of 269 °C (Figure S8).

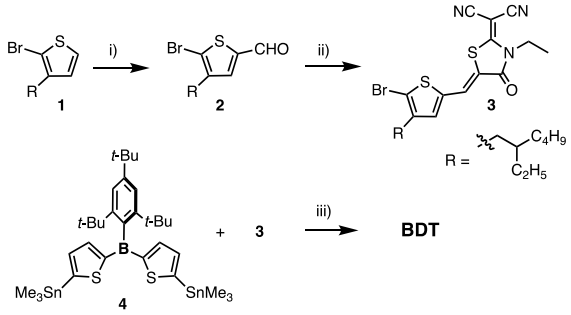

Scheme 1. The synthetic route to **BDT**. Reagents and conditions: i) a) lithium diisopropylamide, tetrahydrofuran, -78 °C, b) N,N-dimethylformamide, r.t.; ii) 2-(3-ethyl-4-oxothiazolidin-2-ylidene)malononitrile, piperidine, chloroform, reflux; iii) $Pd(PPh_3)_4$, CuI, toluene, 115 °C.

We performed density-functional theory (DFT) calculations at the B3LYP/6-31G* level on model compounds of **BDT** and **TT** without the long alkyl chains to investigate the molecular arrangements and electronic structures.[17] As shown in Figure 2b, in the most stable conformation of **BDT**, the sulfur atoms of the two thiophene units on boron both point away from the Mes* group, leading to an axisymmetric configuration. The conjugated backbone of **BDT** adopts a nearly planar conformation, while the Mes* group on the boron atom is oriented almost orthogonal to the backbone. In contrast, in the optimized configuration of **TT**, the sulfur atoms of the central two thiophene units point in opposite directions, resulting in a centrosymmetric configuration. As a result, **BDT** possesses a natural dipole moment of 8.0 Debye, but that of **TT** is only 0.3 Debye.

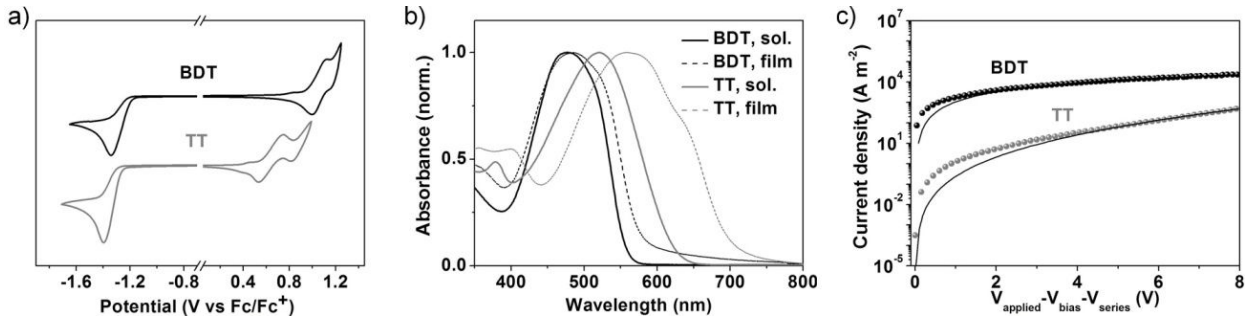

Figure 3. a) Cyclic voltammograms of **BDT** and **TT** in dichloromethane solution. b) UV/vis absorption spectra of **BDT** and **TT** in chlorobenzene (CB) solution and as thin films. c) *J-V* curves and SCLC fittings of the electron-only devices based on **BDT** and **TT** (device structure: ITO/PEIE/BDT or TT/Ca/Al).

Table 1. Photophysical characteristics, electrochemical properties and electron mobilities of **BDT** and **TT**.

	λhexanol max (nm)	εhexanol max (L mol^{-1} cm^{-1})	λCB max (nm)	εCB max (L mol^{-1} cm^{-1})	λfilm max (nm)	*E*opt g (eV)	*E*red onset[a] (V)	*E*ox onset[a] (V)	E_{LUMO} (eV)	E_{HOMO} (eV)	μ_e (cm^2 V^{-1} s^{-1})
BDT	474	4.90×10^4	477	5.80×10^4	487	2.16	-1.19[b]	0.93	-3.61	-5.73	1.37×10^{-5}
TT	-	-	520	6.20×10^4	553	1.79	-1.28	0.53	-3.52	-5.33	4.86×10^{-7}

[a] Onset potential vs. Fc/Fc$^+$ in dichloromethane. [b] The *E*red onset of **BDT** is attributed to the reduction of the terminal groups; the boron-centered reduction would be present at more negative potential.[6c]

To estimate E_{LUMO}/E_{HOMO} of **BDT** and **TT**, we performed cyclic voltammetry (CV) measurements on solutions in dichloromethane. The cyclic voltammograms are shown in Figure 3a. **BDT** and **TT** show both reduction and oxidation waves. According to the onset reduction and oxidation potentials, the E_{LUMO}/E_{HOMO} of **BDT** and **TT** are estimated to be -3.61 eV / -5.73 eV and -3.52 eV / -5.33 eV, respectively (Table 1). The E_{LUMO} and E_{HOMO} of **BDT** are lower than those of **TT** by 0.09 eV and 0.40 eV, respectively. These findings are consistent with the DFT calculation results. As mentioned before, the downshifted E_{LUMO} is due to the p-π* conjugation in the LUMO involving the boron atom and the downshifted E_{HOMO} is due to the node on the boron atom in the HOMO.

Figure 3b shows the absorption spectra of the two compounds in chlorobenzene (CB) solution and as thin films. The photophysical characteristics are listed in Table 1. In solution, the absorption spectrum of **BDT** is blueshifted by 43 nm compared with that of **TT**. This is due to the aforementioned increased bandgap of **BDT**. The absorption band is redshifted upon going from solution to a thin film by 10 nm for **BDT** and 33 nm for **TT**. The small redshift of **BDT** indicates relatively weaker intermolecular interactions of **BDT**, which is due to the steric hindrance effect of the Mes* group on the boron atom.

The electron mobilities of the two compounds were measured using the space-charge-limited-current (SCLC) method using the current density-voltage (*J-V*) curves of electron-only devices shown in Figure 3c. The electron mobilities of **BDT** and **TT** are estimated to be 1.37×10^{-5} cm^2 V^{-1} s^{-1} and 4.86×10^{-7} cm^2 V^{-1} s^{-1}, respectively. The much higher electron mobility of **BDT** in comparison to **TT** could be due to favorable slipped stacking in the solid state. High electron mobilities are frequently observed for acceptor-donor-acceptor (A-D-A) type molecules bearing bulky groups in the core.[19] In these systems, the steric hindrance forces the molecules to adopt a solid state structure, in which terminal A units can stack together to form continuous electron transporting channels for high electron mobility.[18] In **BDT**, the Mes* group on the boron atom is oriented perpendicular to the p-π* conjugated backbone (see Figure 2b), and the resulting steric hindrance may induce the **BDT** molecules to adopt such a slipped stacking pattern that allows for high electron mobility. X-ray diffraction data on thin films, however, did not provide evidence for long range order (Figure S9).

The low-lying E_{LUMO}/E_{HOMO} and high electron mobility indicate that **BDT** acts as an n-type organic semiconductor. This motivated us to test its application as electron acceptor in alcohol-processed OSCs. OSCs are generally processed with halogenated solvent, which is eco-unfriendly, and it is challenging to develop OSCs that can be fabricated with alcohols. To match the alcohol-soluble small molecule acceptor **BDT** with a suitable donor, we followed literature methods and synthesized the alcohol-soluble polymer **D-OEG** (Figure 4b).[9a] The synthesis details are provided in the Supporting Information. Due to the long and branched OEG side chains, **D-OEG** is well soluble in 1-butanol and 1-hexanol. The E_{LUMO}/E_{HOMO} of **D-OEG** is estimated to be -3.39/-4.92 eV, which matches well with those of **BDT** (Figure S10, Supporting Information). The OSC device structure is indium tin oxide (ITO)/poly(3,4-ethylenedioxythiophene) doped with poly(styrenesulfonate) (PEDOT:PSS)/ **D-OEG**:**BDT** /Ca/Al (Figure 4a). The active layer

was spin-coated from a 1-hexanol solution of **D-OEG** and **BDT**. Figures 4c,d show the *J-V* curve under AM1.5G illumination at 100 mW cm^{-2} and the external quantum efficiency (EQE) spectrum of the device. The device shows an open-circuit voltage (V_{OC}) of 1.08 V, short-circuit current density (J_{SC}) of 2.83 mA cm^{-2}, and a fill factor (FF) of 33.6%, corresponding to a power conversion efficiency (PCE) of 1.03%. The EQE spectrum spans from 320 nm to 700 nm with a maximum value of 19%. OSCs based on non-fullerene acceptors are receiving great attention recently and their PCE has increased rapidly to more than 15%.[20] However, to our best knowledge, this is the first report of the successful use of an alcohol-processed non-fullerene electron acceptor in OSCs. The preliminary device results unambiguously prove that **BDT** can be used as an n-type organic semiconductor for alcohol-processable organic opto-electronic devices.

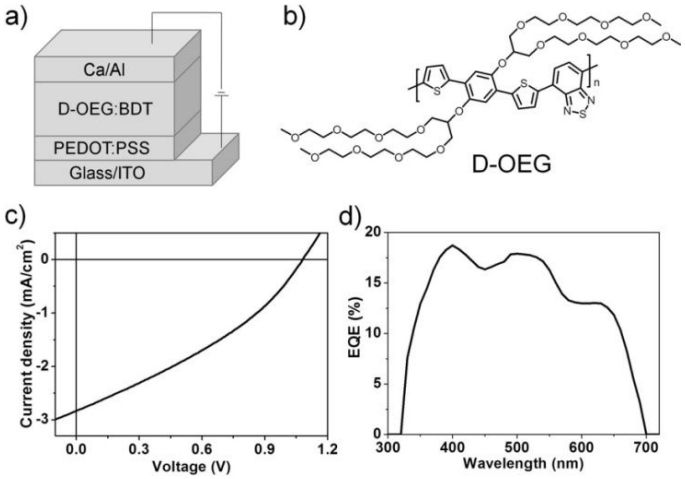

Figure 4. a) Illustration of the device structure based on **D-OEG**:**BDT**. b) The chemical structure of **D-OEG**. c) *J–V* curve and d) EQE spectrum of the OSC device processed with 1-hexanol.

The relatively low PCE of the alcohol-processed OSC device may be due to suboptimal phase separation in the active layer.[21] We measured the surface morphology of neat films and blended active layers using atomic force microscopy (AFM). The AFM height and phase images are shown in Figure S12. The neat film of **BDT** shows spheroidal aggregates with domain sizes of more than 200 nm; the surface root-mean-square (rms) roughness is calculated to be 2.81 nm, which implies that severe aggregation occurs. The neat film of **D-OEG** shows a homogeneous morphology with obvious fibrous networks; the surface rms roughness is calculated to be 0.60 nm. However, for the active layer, consisting of a blend of **BDT** and **D-OEG**, an ordered array of fibers is not observed. A possible reason is that the severe aggregation of **BDT** inhibits the ordering of blends. The amorphous morphology in the active layer is detrimental to the charge carrier transport. Besides, the strong aggregation of **BDT** may lead to local phase separation in the active layer, which likely hampers exciton diffusion and dissociation, leading to the modest J_{SC} and FF. Much improved photovoltaic performance can be expected after optimization of the active layer morphology of the alcohol-processed OSC devices.

Conclusions

In summary, we have developed a p-π* conjugated organoboron molecule as alcohol-processable n-type organic semiconductor. The unique alcohol solubility in the absence of polar side chains is mainly attributed to the large dipole moment and flexibility of the boron-embedded p-π* conjugated backbone. **BDT** exhibits low-lying E_{LUMO}/E_{HOMO} of -3.61 eV / -5.73 eV combined with a high electron mobility of 1.37×10^{-5} cm^2 V^{-1} s^{-1}. We also demonstrate its application in alcohol-processed OSC devices. This work suggests that p-π* conjugation based on triarylboranes is an effective strategy to develop n-type organic semiconductors with interesting electronic structures and unique properties for organic opto-electronic device applications.

Conflicts of interest

There are no conflicts to declare.

Acknowledgements

The authors are grateful for the financial supports by the National Key Basic Research and Development Program of Chi na (973program, Grant No. 2015CB655001). Funded by MOST, the Natural Science Foundation of China (No. 21625403, 21875244, 21875241, 51603203, 21761132020), the Strategic Priority Research Program of Chinese Academy of Sciences (No. XDB12010200). F. J. and A. F. A. thank the US National Science Foundation (NSF) for support under grant CHE-1664975 and A. F. A. thanks the government of Saudi Arabia for a scholarship.

Notes and references

1 a) Z. Zhang, M. Liao, H. Lou, Y. Hu, X. Sun and H. Peng, *Adv. Mater.,* 2018, **30**, 1704261; b) J. Yang, B. Xiao, A. Tang, J. Li, X. Wang and E. Zhou, *Adv. Mater.*, DOI: 10.1002/adma.201804699; c) S. D. Collins, N. A. Ran, M. C. Heiber and T.-Q. Nguyen, *Adv. Energy Mater.,* 2017, **7**, 1602242; d) L. Lu, T. Zheng, Q. Wu, A. M. Schneider, D. Zhao and L. Yu, *Chem. Rev.,* 2015, **115**, 12666-12731; e) A. J. Heeger, *Chem. Soc. Rev.,* 2010, **39**, 2354-2371; f) S. Allard, M. Forster, B. Souharce, H. Thiem and U. Scherf, *Angew. Chem. Int. Ed.,* 2008, **47**, 4070-4098.

2 a) B. Meng, Z. Wang, W. Ma, Z. Xie, J. Liu and L. Wang, *Adv. Funct. Mater.,* 2016, **26**, 226-232; b) E. Wang, W. Mammo and M. R. Andersson, *Adv. Mater.,* 2014, **26**, 1801-1826; c) Z. R. Yi, S. Wang and Y. Q. Liu, *Adv. Mater.,* 2015, **27**, 3589-3606; d) Y. Sun, S. C. Chien, H. L. Yip, Y. Zhang, K. S. Chen, D. F. Zeigler, F. C. Chen, B. P. Lin and A. K. Y. Jen, *Chem. Mater.,* 2011, **23**, 5006-5015; e) H. Yan, P. Lee, N. R. Armstrong, A. Graham, G. A. Evmenenko, P. Dutta and T. J. Marks, *J. Am. Chem. Soc.,* 2005, **127**, 3172-3183.

3 a) Y. Deng, B. Sun, Y. He, J. Quinn, C. Guo and Y. Li, *Angew. Chem. Int. Ed.*, 2016, **55**, 3459-3462; b) Z. Yuan, B. Fu, S. Thomas, S. Zhang, G. DeLuca, R. Chang, L. Lopez, C. Fares, G. Zhang, J.-L. Bredas and E. Reichmanis, *Chem. Mater.*, 2016, **28**,

6045-6049; c) T. Lei, J.-H. Dou, X.-Y. Cao, J.-Y. Wang and J. Pei, *J. Am. Chem. Soc.*, 2013, **135**, 12168-12171; d) C. Zhang, Y. Zang, E. Gann, C. R. McNeill, X. Zhu, C.-A. Di and D. Zhu, *J. Am. Chem. Soc.*, 2014, **136**, 16176-16184; e) B. Meng, J. Miao, J. Liu and L. Wang, *Macromol. Rapid Commun.*, 2018, **39**, 1700505; f) C. Dou, J. Liu and L. Wang, *Sci. China Chem.*, 2017, **60**, 450-459.

4 a) M. Stolar and T. Baumgartner, *Phys. Chem. Chem. Phys.,* 2013, **15**, 9007-9024; b) X. M. He and T. Baumgartner, *RSC Adv.,* 2013, *3*, 11334-11350; c) A. M. Priegert, B. W. Rawe, S. C. Serin and D. P. Gates, *Chem. Soc. Rev.,* 2016, **45**, 922-953; d) D. Joly, P. A. Bouit and M. Hissler, *J. Mater. Chem. C,* 2016, **4**, 3686-3698; e) M. Stępień, E. Gońka, M. Żyła and N. Sprutta, *Chem. Rev.,* 2017, **117**, 3479-3716; f) G. Zhang, J. Zhao, P. C. Y. Chow, K. Jiang, J. Zhang, Z. Zhu, J. Zhang, F. Huang and H. Yan, *Chem. Rev.,* 2018, **118**, 3447-3507; g) F. Vidal and F. Jäkle, *Angew. Chem. Int. Ed.,* 2019, **58**, 5846-5870.

5 a) N. Matsumi, K. Naka and Y. Chujo, *J. Am. Chem. Soc.*, 1998, **120**, 5112-5113; b) S. Cataldo, S. Fabiano, F. Ferrante, F. Previti, S. Patanè and B. Pignataro, *Macromol. Rapid Commun.,* 2010, **31**, 1281-1286; c) B. Meng, Y. Ren, J. Liu, F. Jäkle and L. Wang, *Angew. Chem. Int. Ed.,* 2018, **57**, 2183-2187; b) d) G. R. Kumar, S. K. Sarkar and P. Thilagar, *Chem.-Eur. J.,* 2016, **22**, 17215-17225; e) T. A. Welsh, A. Laventure, A. F. Alahmadi, G. Zhang, T. Baumgartner, Y. Zou, F. Jäkle, G. C. Welch, *ACS Appl. Energy Mater.* 2019, **2**, 1229-1240.

6 a) X. D. Yin, J. W. Chen, R. A. Lalancette, T. B. Marder and F. Jäkle, *Angew. Chem. Int. Ed.,* 2014, **53**, 9761-9765; b) X. D. Yin, F. Guo, R. A. Lalancette and F. Jäkle, *Macromolecules,* 2016, **49**, 537-546; c) X. Yin, K. Liu, Y. Ren, R. A. Lalancette, Y.-L. Loo and F. Jäkle, *Chem. Sci.,* 2017, **8**, 5497-5505; d) J. F. Chai, C. Wang, L. Jia, Y. Pang, M. Graham and S. Z. D. Cheng, *Synth. Met.,* 2009, **159**, 1443-1449; e) Z. M. Hudson, C. Sun, M. G. Helander, Y.-L. Chang, Z.-H. Lu and S. Wang, *J. Am. Chem. Soc.*, 2012, **134**, 13930-13933; f) T. Kushida, A. Shuto, M. Yoshio, T. Kato and S. Yamaguchi, *Angew. Chem. Int. Ed.,* 2015, **54**, 6922-6925; g) S. Brend'amour, J. Gilmer, M. Bolte, H.-W. Lerner and M. Wagner, *Chem. Eur. J.,* 2018*,* **24,** 16910-16918; h) A. Lik, S. Jenthra, L. Fritze, L. Müller, K.-N. Truong and H. Helten *Chem. Eur. J.,* 2018, **24**, 11961-11972; i) S. Muhammad, M. R. S. A. Janjua, Z. Su, *J. Phys. Chem. C*, 2009, **113**, 12551-12557.

7 Reviews: a) C. D. Entwistle and T. B. Marder, *Angew. Chem. Int. Ed.,* 2002, **41**, 2927-2931; b) C. D. Entwistle and T. B. Marder, *Chem. Mater.,* 2004, **16**, 4574-4585; c) F. Jäkle, *Chem. Rev.,* 2010, **110**, 3985-4022; d) Z. M. Hudson and S. Wang *Dalton Trans*., 2011, **40**, 7805-7816; e) A. Lorbach, A. Hübner and M. Wagner, *Dalton Trans.,* 2012, **41**, 6048-6063; f) K. Tanaka and Y. Chujo, *Macromol. Rapid Comm.*, 2012, **33**, 1235-1255; g) A. Wakamiya and S. Yamaguchi, *Bull. Chem. Soc. Jpn.,* 2015, **88**, 1357-1377; h) Y. Ren and F. Jäkle, *Dalton Trans.,* 2016, **45**, 13996-14007; i) S. Mukherjee and P. Thilagar, *J. Mater. Chem. C,* 2016, **4**, 2647-2662; j) L. Ji, S. Griesbeck and T. B. Marder, *Chem. Sci.,* 2017, **8**, 846-863; k) E. von Grotthuss, A. John, T. Kaese and M. Wagner, *Asian J. Org. Chem.,* 2018, **7**, 37-53; l) J. H. Huang and Y. Q. Li, *Front. Chem.,* 2018, **6**, 341.

8 a) T. Lei, J. Y. Wang and J. Pei, *Chem. Mater.,* 2014, **26**, 594-603; b) J. Mei and Z. Bao, *Chem. Mater.,* 2014, **26**, 604-615; c) B. Meng, Y. Fu, Z. Xie, J. Liu and L. Wang, *Macromolecules,* 2014, **47**, 6246-6251; d) B. Meng, H. Song, X. Chen, Z. Xie, J. Liu and L. Wang, *Macromolecules,* 2015, **48**, 4357-4363.

9 a) T. L. Nguyen, C. Lee, H. Kim, Y. Kim, W. Lee, J. H. Oh, B. J. Kim and H. Y. Woo, *Macromolecules,* 2017, **50**, 4415-4424; b) Y. Kim, J. Choi, C. Lee, Y. Kim, C. Kim, T. L. Nguyen, B. Gautam, K. Gundogdu, H. Y. Woo and B. J. Kim, *Chem. Mater.,* 2018, **30**, 5663-5672; c) C. Lee, H. R. Lee, J. Choi, Y. Kim, T. L. Nguyen, W. Lee, B. Gautam, X. Liu, K. Zhang, F. Huang, J. H. Oh, H. Y. Woo and B. J. Kim, *Adv. Energy Mater.*, 2018, **8**, 1802674; d) C. H. Duan, W. Z. Cai, B. B. Y. Hsu, C. M. Zhong, K. Zhang, C. C. Liu, Z. C. Hu, F. Huang, G. C. Bazan, A. J. Heeger and Y. Cao, *Energy Environ. Sci.,* 2013, **6**, 3022-3034.

10 a) T. Yu, X. Xu, G. Zhang, J. Wan, Y. Li and Q. Peng, *Adv. Funct. Mater.*, 2017, **27**, 1701491; b) H. S. Xin, C. W. Ge, X. C. Jiao, X. D. Yang, K. Rundel, C. R. McNeill and X. K. Gao, *Angew. Chem. Int. Ed.,* 2018, **57**, 1322-1326; c) J. Miao, B. Meng, J. Liu and L. Wang, *Chem. Commun.,* 2018, **54**, 303-306; d) Z.-G. Zhang, Y. Li, L. Zhong, B. Gautam, H. Bin, J.-D. Lin, F.-P. Wu, Z. Zhang, K. Gundogdu, Y. Li, Z.-Q. Jiang and L. S. Liao, *Energy Environ. Sci.,* 2017, **10**, 1610-1620.

11 a) T. R. Andersen, T. T. Larsen-Olsen, B. Andreasen, A. P. L. Bottiger, J. E. Carle, M. Helgesen, E. Bundgaard, K. Norrman, J. W. Andreasen, M. Jorgensen and F. C. Krebs, *ACS Nano,* 2011, **5**, 4188-4196; b) P. G. Jessop, *Green Chem.,* 2011, **13**, 1391-1398.

12 a) C. Qin, Y. Cheng, L. Wang, X. Jing and F. Wang, *Macromolecules,* 2008, **41**, 7798-7804; b) B. H. Zhang, C. J. Qin, X. D. Niu, Z. Y. Xie, Y. X. Cheng, L. X. Wang and X. L. Li, *Appl. Phys. Lett.,* 2010, **97**, 043506.

13 a) B. Xu, Z. Zheng, K. Zhao and J. Hou, *Adv. Mater.,* 2016, **28**, 434-439; b) B. Xu and J. Hou, *Adv. Energy Mater.*, 2018, **8**, 1800022.

14 a) F. Huang, H. Wu, D. Wang, W. Yang and Y. Cao, *Chem.* Mater.*,* 2004, **16**, 708-716; b) Z. Wu, C. Sun, S. Dong, X.-F. Jiang, S. Wu, H. Wu, H.-L. Yip, F. Huang and Y. Cao, *J. Am. Chem. Soc.,* 2016, **138**, 2004-2013; c) J. Jia, B. Fan, M. Xiao, T. Jia, Y. Jin, Y. Li, F. Huang and Y. Cao, *Macromolecules,* 2018, **51**, 2195-2202.

15 a) F. Liu, Z. Zhou, C. Zhang, T. Vergote, H. Fan, F. Liu and X. Zhu, *J. Am. Chem. Soc.,* 2016, **138**, 15523-15526; b) S. Xu, Z. Zhou, H. Fan, L. Ren, F. Liu, X. Zhu and T. P. Russell, *J. Mater. Chem. A,* 2016, **4**, 17354-17362; c) P. Ye, Y. Chen, J. Wu, X. Wu, S. Yu, X. Wang, Q. Liu, X. Jia, A. Peng and H. Huang, *J. Mater. Chem. C,* 2017, **5**, 12591-12596.

16 a) N. Gasparini, A. Wadsworth, M. Moser, D. Baran, I. McCulloch and C. J. Brabec, *Adv. Energy Mater.*, 2018, **8**, 1703298; b) H. Bin and Y. Li, *Acta Polym. Sin.,* 2017, **9**, 1444-1461; c) J. J. Feng, W. Jiang and Z. H. Wang, *Chem. Asian J.,* 2018, **13**, 20-30.

17 DFT calculations were performed using Gaussian 09: M. J. Frisch, et al. Gaussian 09, revision A.02; Gaussian, Inc.: Wallingford, CT, 2009. For details, see the Supporting Information.

18 a) G. Han, Y. Guo, X. Song, Y. Wang and Y. Yi, *J. Mater. Chem. C,* 2017, **5**, 4852-4857; b) H. Yao, L. Ye, J. Hou, B. Jang, G. Han, Y. Cui, G. M. Su, C. Wang, B. Gao, R. Yu, H. Zhang, Y. Yi, H. Y. Woo, H. Ade and J. Hou, *Adv. Mater.,* 2017, **29**, 1700254.

19 a) W. Gao, M. Zhang, T. Liu, R. Ming, Q. An, K. Wu, D. Xie, Z. Luo, C. Zhong, F. Liu, F. Zhang, H. Yan and C. Yang, *Adv. Mater.,* 2018, **30**, 1800052. b) Y. Z. Lin, J. Y. Wang, Z. G. Zhang, H. T. Bai, Y. F. Li, D. B. Zhu and X. W. Zhan, *Adv. Mater.,* 2015, **27**, 1170-1174; c) Y. Liu, Z. Zhang, S. Feng, M. Li, L. Wu, R. Hou, X. Xu, X. Chen and Z. Bo, *J. Am. Chem. Soc.,* 2017, **139**, 3356-3359.

20 J. Yuan, Y. Zhang, L. Zhou, G. Zhang, H.-L. Yip, T.-K. Lau, X. Lu, C. Zhu, H. Peng, P. A. Johnson, M. Leclerc, Y. Cao, J. Ulanski, Y. Li and Y. Zou, *Joule,* 2019, doi: 10.1016/j.joule.2019.01.004.

21 a) B. C. Thompson and J. M. J. Frechet, *Angew. Chem. Int. Ed.,* 2008, **47**, 58-77; b) C. J. Brabec, M. Heeney, I. McCulloch and J. Nelson, *Chem. Soc. Rev.,* 2011, **40**, 1185-1199; c) M. T. Dang, L. Hirsch, G. Wantz and J. D. Wuest, *Chem. Rev.,* 2013, **113**, 3734-3765.

Entry for the Table of Contents

A p-π* Conjugated Triarylborane as an Alcohol-Processable n-Type Semiconductor for Organic Optoelectronic Devices

Yingjian Yu, Changshuai Dong, Abdullah F. Alahmadi, Bin Meng,* Jun Liu,* Frieder Jäkle* and Lixiang Wang

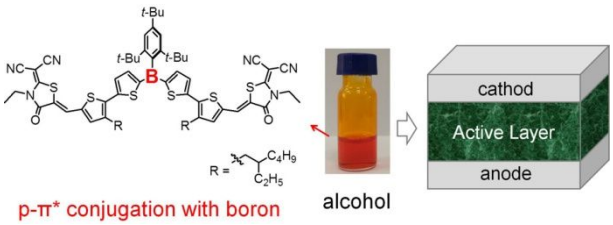

A new n-type p-π* conjugated organic molecule based on triarylborane shows unique alcohol-solubility even in the absence of polar side chains. With its low-lying LUMO/HOMO energy levels and high electron mobility, the molecule can be used as electron acceptor in eco-friendly alcohol-processed organic solar cells.